# In-the-Field Calibration of All-Digital MIMO Arrays

Maryam Eslami Rasekh*, Bhagyashree Puranik†, Upamanyu Madhow‡, Mark Rodwell§

*Dept. of Electrical and Computer Engineering*
*University of California Santa Barbara*
Santa Barbara, California 93106
Email: {*rasekh, †bpuranik, ‡madhow, §rodwell}@ece.ucsb.edu

***Abstract*—A key goal of next generation networks is to scale hardware design and signal processing algorithms to mmWave and THz arrays with a large number of elements. Imperfect manufacturing and limitations of circuit design introduce variations in the gain and relative phase offset of transmit and receive array elements that must be compensated prior to beam formation for either communication or sensing. We propose a novel method for calibrating large arrays in the field by exploiting the sparsity of the spatial channel. While conventional calibration methods are susceptible to multipath components in the wireless channel, our approach is shown to be robust to multipath interference if the number of measurement locations is sufficiently large.**

***Index Terms*—Array calibration, digital beamforming, massive MIMO, reciprocity, millimeter wave, THz**

## I. Introduction

As emerging technologies look to millimeter wave (mmWave) and Terahertz (THz) frequencies for higher bandwidth and spatial reuse, massive MIMO architectures play a crucial role in realizing these gains. As the wavelength shrinks to sub-centimeter lengths, hundreds, or even thousands, of elements can be packed together on compact platforms, providing high beamforming gain, interference suppression, and, in the case of digitally controlled arrays, spatial multiplexing. However, manufacturing can be more challenging at small wavelengths, as small variations in RF circuitry and local oscillator distribution paths can cause large, unpredictable variations in the RF chain response of different array elements. At THz frequencies, even sub-millimeter path differences can produce very large phase shifts, causing completely random phase offsets across the transmitter and receiver arrays. As a result, the spatial channels in uplink and downlink are effectively multiplied by different random vectors that. As illustrated in Fig. 1, this disrupts the geometric reciprocity and spatial frequency domain sparsity of the channel, on which many algorithms rely for MIMO processing and denoising [1], [2]. Thus, an important prerequisite for taking advantage of the dimensionality gains provided by massive MIMO for communication and sensing is to accurately estimate these offsets and compensate for them in the digital backend.

This work was supported in part by ComSenTer, one of six centers in JUMP, a Semiconductor Research Corporation (SRC) program sponsored by DARPA.

Conventionally, array calibration is performed in a controlled environment (e.g., anechoic chamber where a pure single path channel is guaranteed) by exciting the array from a source in its boresight. In these conditions, the channel response is constant on the array antennas and the measured signal is the calibration vector itself. This procedure is costly and time consuming and its accuracy may be degraded by slight changes in calibration offsets over time, e.g., due to environmental effects or other sources of stress.

**Contributions:** We propose a framework for *post-deployment* uplink and downlink calibration of a base station array in an uncontrolled multipath environment. Our procedure relies on gathering over-the-air measurements from several sources (mobiles or nearby base stations) at different locations for joint calibration and spatial channel estimation. We exploit this location diversity to mitigate distortion due to multipath via an "align and average" strategy for the line of sight (LOS) paths[1] as follows:

- First, the pairwise spatial frequency difference between the LOS components of measurements is estimated by conjugate multiplication and compressive estimation of the dominant frequency.
- All measurements are derotated such that their LOS directions are aligned.
- The strongest eigenvector of the aligned measurements is calculated via spectral decomposition to obtain an initial estimate of the calibration vector.
- The estimate is refined by reconstructing the full multipath channel at each location using sparse estimation techniques and estimating the calibration vector from the original measurements conditioned on the channels.

We observe that even strong multipath can be filtered out using as few as 10 measurements using this technique, provided the measurements have sufficiently high SNR. For the algorithm to succeed, there is a minimum requirement on the *per-element* SNR, which, when scaling to large arrays designed for beamformed communication, requires the measurements to aggregate signal power over a time interval that scales linearly with array size. In downlink (transmitter calibration), this

[1]While we use the term LOS for the dominant path, our approach may also apply in scenarios with LOS blockage if there is a strong reflected path.

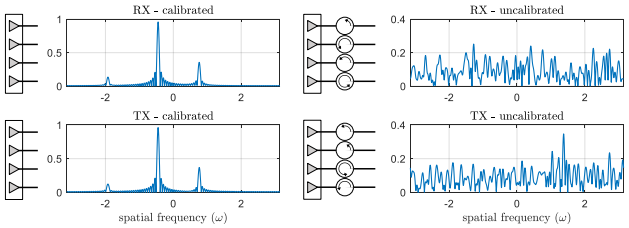


Fig. 1. Disruption of channel sparsity and reciprocity by calibration offsets.

aggregation happens automatically as orthogonal sequences must be transmitted on different array elements to measure the full channel vector, necessitating a minimum sequence length of $N_{\text{tx}}$. For uplink calibration, we show that geometric reciprocity, i.e., equivalence of angle of departure (AOD) and angle of arrival (AOA) for each path in the channel, can be leveraged to significantly relax the SNR requirement by "piggybacking" on downlink calibration. Our results show that this approach can reduce the minimum required SNR by around 20 dB for a 100 element antenna.

**Related work:** Calibration of RF chains has long been of interest, mainly for the goal of extending channel reciprocity to end-to-end uplink-downlink reciprocity. One approach used in the literature is to include dedicated hardware inside the RF circuitry for calibration. For instance, in [3], extra elements are added to the array that are not supported by a full RF chain and act as pilot transmitters for calibration. A more scalable and cost-efficient approach is to use external sources, either in controlled environments with a known channel response, as in [4], [5], or by jointly estimating the channel and calibration offsets. Without relying on the channel sparsity assumption, joint calibration and channel estimation requires many measurements and a high level of coordination between transmit and receive arrays [6]. In [7], the authors assume single path channels between the source and receiver and perform joint direction of arrival estimation and broadband calibration. Second order statistics are used in [8]–[10] to derive array offset parameters. These rely on a set of sources with single-path channels transmitting unknown but uncorrelated signals over time, utilizing the information in the observed covariance matrix for estimation of array gain and phase offsets, which are in turn used to estimate the AOA of each source. These techniques rely on rotational invariance of the source channels and therefore only apply to single path channels that excite only one spatial frequency on the array. In the presence of multipath, the performance of these methods is severely degraded, as we show in section V. With large enough bandwidth, multipath components can be separated in time, and the direction and delay of each path can be estimated jointly with array offsets. This approach is used in [11] for joint calibration and delay estimation using a wideband OFDM sequence. To the best of our knowledge, the only prior work that attempts blind calibration in the presence of multipath is [12] wherein the authors propose a semi-definite programming based convex optimization framework for joint estimation

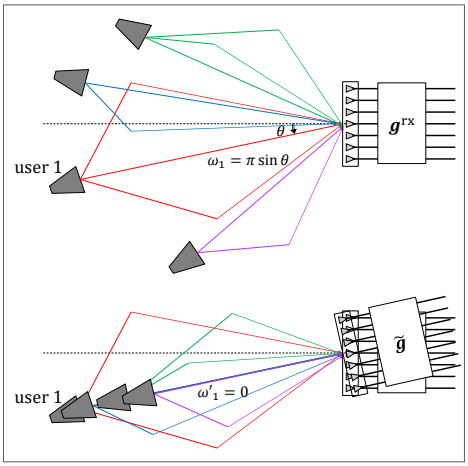


Fig. 2. Rotation of angular reference perception toward direction of user 1 and alignment of LOS components of channels with that of channel 1

of sparse channels and calibration coefficients. However, the computational complexity of this method for an array of length $N$ is $\mathcal{O}(N^3)$ making it a poor match for massive MIMO arrays. Here, we propose a scalable blind calibration algorithm that is robust to multipath, and therefore suitable for continuous in-the-field calibration.

## II. System Model

The base station consists of separate, digitally-controlled transmit and receive arrays with $N_{\text{tx}}$ and $N_{\text{rx}}$ elements, respectively. In our analysis we assume $N_{\text{tx}} = N_{\text{rx}} = N$, and that both arrays are linear with half wavelength spacing. The nominal response vector for a unit-amplitude plane wave incident from angle $\theta$ is therefore described as

$$\mathbf{r}(\theta) = \left[1, e^{j\pi \sin\theta}, e^{j2\pi \sin\theta}, \ldots, e^{j(N_{\text{rx}}-1)\pi \sin\theta}\right]^T. \quad (1)$$

We denote with $\omega = \pi \sin\theta$ the equivalent *spatial frequency* to angle of arrival $\theta$, and use them interchangeably. Assuming the user is far away from the base station, any single-path channel excites the same spatial frequency in uplink and downlink, but with a constant phase shift due to the relative displacement of the arrays. This phase shift varies depending on the angle of incidence, meaning conventional channel reciprocity does not hold for *multipath* channels. However, *geometric* reciprocity still guarantees that the angles of departure and arrival are the same for each path in the channel. Thus, despite the absence of full channel reciprocity for displaced arrays, geometric reciprocity (or path reciprocity) can be relied upon when beamforming toward the strongest direction in the channel–provided the arrays are *calibrated*.

We denote the uplink (receiver) and downlink (transmitter) calibration vectors by $\mathbf{g}^{\text{rx}}$ and $\mathbf{g}^{\text{tx}}$, respectively, and our goal is to estimate these coefficients, up to a constant phase and spatial frequency offset, via a simple training procedure. We first focus on receiver calibration and later discuss how the framework can be applied to transmitter calibration.

The phase and amplitude of received signals are altered by the receiver calibration vector,

$$\mathbf{g}^{\text{rx}}[n] = \alpha_n e^{j\phi_n}, \tag{2}$$

where $\alpha_n \in \mathbb{R}^+, \phi_n \in [0, 2\pi)$. Thus, a unit-amplitude single-path channel with angle of arrival $\theta$ (or spatial frequency $\omega$) would result in the received signal vector

$$\mathbf{y}(\omega) = \text{diag}(\mathbf{g}^{\text{rx}})\mathbf{r}(\omega), \tag{3}$$

with $\mathbf{y}[n] = \mathbf{g}^{\text{rx}}[n]e^{jn\omega} = \alpha_n e^{j(n\omega+\phi_n)}, n = 0, ..., N_{\text{rx}} - 1$. To recover the uplink calibration vector, we rely on a set of $M$ channel measurements from users dispersed in the cell (or other nearby base stations). Source $m$ is located at direction $\theta_m$ (or spatial frequency $\omega_m$), and therefore its LOS produces the normalized response vector $\text{diag}(\mathbf{g}^{\text{rx}})\mathbf{r}(\omega_m)$. The channel measurement vector from location $m$ is therefore equal to

$$\begin{aligned}\mathbf{y}_m &= \text{diag}(\mathbf{g}^{\text{rx}})\mathbf{h}_m + \boldsymbol{\nu}_m \\ &= a_m \text{diag}(\mathbf{g}^{\text{rx}})\mathbf{r}(\omega_m) && \leftarrow (\text{LOS}_m) \\ &+ \text{diag}(\mathbf{g}^{\text{rx}}) \sum_{k=1}^{K_m} a'_{m,k}\mathbf{r}(\omega'_{m,k}) && \leftarrow (\text{MP}_m) \\ &+ \boldsymbol{\nu}_m && \leftarrow (\text{noise})\end{aligned} \tag{4}$$

where $a_m$ and $\omega_m$ are the complex amplitude and spatial frequency of the LOS path for user $m$, $K_m$ is the number of multipath components in channel $m$, $a'_{m,k}$ and $\omega'_{m,k}$ are the complex amplitude and spatial frequency of the $k$'th multipath component of user $m$, and $\boldsymbol{\nu}_m \sim \mathcal{CN}(\mathbf{0}, \sigma^2\mathbf{I})$ is the receiver noise vector. We use the notation $\text{MP}_m$ as a shorthand for the total contribution of non line of sight (NLOS) multipath components, which is typically smaller than the LOS contribution. We initially treat this term as noise (and treat all channels as single path), and later use sparse estimation techniques to recover the multipath and refine our calibration.

*Angular reference ambiguity*

Assuming all measurements are from single-path channels, finding the calibration coefficients requires joint estimation of source channels, i.e., the directions, $\{\omega_m\}$, and amplitudes, $\{a_m\}$, and the calibration parameters, $\{\mathbf{g}^{\text{rx}}[n] = \alpha_n e^{j\phi_n}\}$, from measurement vectors $\{\mathbf{y}_m\}$. For a given solution, $\mathcal{S} = (\{\alpha_n, \phi_n\}, \{(\omega_m, a_m)\})$, to the measurement equations, and constants $c_1, c_2, c_3$, the set of values

$$\mathcal{S}' = \left(\{\frac{\alpha_n}{c_1}, \phi_n + c_2 + c_3 n\}, \{(\omega_m - c_3, c_1 a_m e^{-jc_2})\}\right) \tag{5}$$

is an equally valid solution, which we express as $\mathcal{S}' \overset{\mathbf{y}}{\equiv} \mathcal{S}$. Here, $c_1$ is the unknown gain scaling, $c_2$ is the unknown phase offset (both of which can be attributed arbitrarily to the wireless channel or the RF chain), and $c_3$ is the ambiguity in angular reference (or "antenna orientation") which cannot be obtained without ground truth information about the true direction of at least one source. Any estimate that is equivalent to the true calibration vector within this definition is a valid solution, as these reference offsets do not affect beamforming or MIMO performance (they do, however, need to be resolved for localization applications where exact knowledge of the orientation of the base station antenna is crucial).

Thus we see that taking one high-SNR measurement from a single location is sufficient for obtaining the calibration parameters up to a constant spatial frequency, gain, and phase offset - as long as the channel from that location is a pure line of sight that excites *only one frequency* on the array. As this is not the case in deployment environments, we propose the following algorithm for calibration in the presence of multipath.

## III. Algorithm

In this section, we describe our algorithm for joint estimation of calibration coefficients and channels using measurements from $M$ user locations. We first consider the uplink direction (receiver calibration) and then discuss how the framework is applied in the downlink for transmitter calibration.

Let us first consider the case where we have noise-free measurements from one source with a single-path channel at direction $\omega_1$,

$$\mathbf{y}_1 = a_1 \text{diag}(\mathbf{g}^{\text{rx}})\mathbf{r}(\omega_1) = \left[a_1\alpha_n e^{j(\phi_1+n\omega_1)}\right]_{n=0:N_{\text{rx}}-1}.$$

Taking $\omega'_1 = 0, a'_1 = 1$, this vector is "equivalent" to the calibration vector $\mathbf{g}^{\text{rx}}$, i.e.,

$$(\mathbf{g}^{\text{rx}}, \{(\omega_1, a_1)\}) \overset{\mathbf{y}}{\equiv} (\tilde{\mathbf{g}} = \mathbf{y}_1, \{(\omega'_1, a'_1)\}).$$

We can therefore take

$$\begin{aligned}\hat{\alpha}_n &= |\mathbf{y}_1[n]| = |a_1|\alpha_n, \\ \hat{\phi}_n &= \angle\mathbf{y}_1[n] = \phi_n + \angle a_1 + n\omega_1, \\ \hat{\omega}_1 &= 0, \quad \hat{a}_1 = 1.\end{aligned}$$

Recall that estimating the calibration vector at a constant frequency offset is sufficient for recovering reciprocity and channel sparsity, and only results in an angular shift in the perception of the antenna about its orientation, as depicted in the illustration of Fig. 2. In our proposed algorithm, we take the LOS of the first measurement as our perceived angular origin (reference) and define

$$\tilde{\mathbf{g}} = a_1 \text{diag}(\mathbf{g}^{\text{rx}})\mathbf{r}(\omega_1), \tag{6}$$

so that

$$\mathbf{y}_1 = \tilde{\mathbf{g}} + \text{MP}_1 + \boldsymbol{\nu}_1. \tag{7}$$

For a second measurement vector $\mathbf{y}_2$ with LOS at angle $\omega_2$, we observe the equivalence,

$$(\mathbf{g}^{\text{rx}}, \{(\omega_1, a_1), (\omega_2, a_2)\}) \overset{\mathbf{y}}{\equiv} \left(\tilde{\mathbf{g}}, \{(0, 1), (\omega_2 - \omega_1, \frac{a_2}{a_1})\}\right).$$

Similarly, any new measurement can be transferred to the reference frame of $\tilde{\mathbf{g}}$ by replacing its LOS angle, $\omega_m$, with the difference $\omega_m - \omega_1$, and dividing its gain, $a_m$, by the gain of the first path to get $a_m/a_1$. We refer to this process as "aligning" measurement $m$ with the reference. The proposed calibration procedure proceeds as follows.

### A. Estimating LOS frequencies in reference frame

The frequency difference and gain ratio between the LOS paths of source $m$ and source 1 can be estimated from non-calibrated measurements $\mathbf{y}_m$ and $\mathbf{y}_1$ by forming the vector

$$\begin{aligned}\mathbf{z}_m &= \left[e^{j(\angle \mathbf{y}_m[n]-\angle \mathbf{y}_1[n])}\right]_{n=0:N_{\text{rx}}-1} \\ &= \left[e^{j((\phi_n+n\omega_m+\angle a_m)-(\phi_1+n\omega_1+\angle a_1))}\right]_{n=0:N_{\text{rx}}-1} \\ &= \left[e^{j(n(\omega_m-\omega_1)+\angle a_m-\angle a_1)}\right]_{n=0:N_{\text{rx}}-1} \end{aligned} \tag{8}$$

and identifying the strongest frequency in this vector, $\omega_m-\omega_1$, using an off-grid frequency estimation algorithm such as Newtonized orthogonal matchin pursuit (NOMP) [13]. After undoing the frequency offset between the two vectors, we can average their element-wise amplitude ratios to find $a_m/a_1$. While (8) is a suitable way to construct $\mathbf{z}_m$ for noiseless and purely LOS channels, in a realistic environment it is better to first undo the absolute gain offsets using a coarse gain estimate (e.g., $\hat{\mathbf{g}}_0[n] = \frac{1}{M}\sum_m |\mathbf{y}_m[n]|$) and then element-wise multiply $\mathbf{y}_m$ by the conjugate of $\mathbf{y}_1$ to produce

$$\mathbf{z}_m[n] = \frac{\mathbf{y}_m[n]\mathbf{y}_1^*[n]}{\hat{\mathbf{g}}_0^2[n]}. \tag{9}$$

This way, the main term in $\mathbf{z}_m$ (element-wise conjugate product of LOS components) is well separated from the multipath components in frequency domain, and the largest frequency identified by NOMP will not be significantly distorted by multipath.

### B. Aligning measurements

After estimating $\omega_m - \omega_1$ for all $m$, we align the (uncalibrated) LOS of all measurements with that of $\mathbf{y}_1$ by undoing this frequency offset, i.e.,

$$\begin{aligned}\tilde{\mathbf{y}}_m[n] &= \mathbf{y}_m[n]e^{-j(\omega_m-\omega_1)n} \\ &= \frac{a_m}{a_1}\mathbf{g}^{\text{rx}}[n]e^{j\omega_1 n} + \text{MP}_m[n]e^{j(\omega_m-\omega_1)n} + \boldsymbol{\nu}'_m[n] \\ &= \frac{a_m}{a_1}\tilde{\mathbf{g}}[n] + \text{MP}'_m + \boldsymbol{\nu}'_m[n]. \end{aligned} \tag{10}$$

This procedure is also illustrated in Fig. 2. Note that these vectors are weighted copies of $\tilde{\mathbf{g}}$ distorted by independent noise and multipath.

### C. Averaging

We now form the $N_{\text{rx}} \times M$ matrix,

$$\mathbf{G} = [\tilde{\mathbf{y}}_1\ \tilde{\mathbf{y}}_2\ ...\ \tilde{\mathbf{y}}_M]. \tag{11}$$

By performing singular value decomposition (SVD) on $\mathbf{G}$ and taking the strongest left eigenvector,

$$\hat{\mathbf{g}} = \mathbf{u}_1(\mathbf{G}), \tag{12}$$

we arrive at our estimate for the (rotated) calibration vector $\tilde{\mathbf{g}}$. As the multipath distortion in different $\tilde{\mathbf{y}}$ vectors will be independent while the LOS components are aligned, increasing the number of measurements $M$ rapidly improves the accuracy of $\hat{\mathbf{g}}$, as we demonstrate numerically in section V.

### D. Refinement via sparse channel reconstruction

We can further refine our estimate of $\tilde{\mathbf{g}}$ by calibrating the original measurements with the output of (12) and obtaining estimates of all of the significant paths in each channel, $\{\hat{a}_m, \hat{\omega}_m, \hat{a}_{m,k}, \hat{\omega}_{m,k}\}$, via a compressive estimation algorithm. We then construct the full channel at each location as

$$\hat{\mathbf{h}}_m = \hat{a}_m \mathbf{r}(\hat{\omega}_m) + \sum_{k=1}^{K_m} \hat{a}_{m,k}\mathbf{r}(\hat{\omega}_{m,k}) \tag{13}$$

and undo it in the original measurements to arrive at a new, more accurate set of vectors,

$$\tilde{\mathbf{y}}'_m[n] = \frac{\mathbf{y}_m[n]}{\hat{\mathbf{h}}_m[n]}, \quad m \in \{1, ..., M\}. \tag{14}$$

We then form the refined matrix,

$$\mathbf{G}' = [\tilde{\mathbf{y}}'_1\ ...\ \tilde{\mathbf{y}}'_M] \tag{15}$$

and perform SVD to arrive at a refined estimate of $\tilde{\mathbf{g}}$,

$$\hat{\mathbf{g}}' = \mathbf{u}_1(\mathbf{G}'). \tag{16}$$

This step can significantly reduce the calibration estimation error provided the initial estimate is sufficiently accurate.

**Transmitter calibration:** Downlink calibration is analogous to uplink, and the same procedure can be used to find $\tilde{\mathbf{g}}^{\text{tx}}$ from $M$ measurements of the uncalibrated downlink channel. To obtain these measurements, the base station broadcasts orthogonal training sequences, e.g., baseband OFDM subcarriers, on its transmit array elements, and the users correlate the observed signals against each sequence to recover the $N_{\text{tx}}$-dimensional measurement vectors, which are provided as feedback. We note that, for effective calibration, it is vital that both the trasmitter and the receiver use *the same path of the same user* as their reference direction, so that $\tilde{\mathbf{g}}^{\text{tx}}$ and $\tilde{\mathbf{g}}^{\text{rx}}$ are consistent in their perceived orientation, and path reciprocity is upheld.

## IV. Scaling and SNR requirement

While increasing the number of measurement locations improves estimation accuracy by averaging multipath and noise, the SNR of each measurement is a significant bottleneck in the success of the algorithm, specifically, the frequency difference estimation step of III-A. To quantify this bottleneck, consider two standard, unit-amplitude complex sinusoids, $\mathbf{x}_1[n] = e^{jn\omega_1}$ and $\mathbf{x}_2[n] = e^{jn\omega_2}$, of length $N$, distorted by complex Gaussian noise, $\boldsymbol{\nu}$, of variance $\sigma^2$. The per-entry SNR of each of these signals is $1/\sigma^2$. The frequency difference is found by multiplying the first vector by the conjugate of the second vector to obtain

$$\begin{aligned}\mathbf{z}[n] &= (\mathbf{x}_1[n] + \boldsymbol{\nu}_1[n])(\mathbf{x}_2[n] + \boldsymbol{\nu}_2[n])^* \\ &= \mathbf{x}_1[n]\mathbf{x}_2^*[n] + (\boldsymbol{\nu}_1[n]\mathbf{x}_2^*[n] \\ &\qquad + \boldsymbol{\nu}_2^*[n]\mathbf{x}_1[n]) + \boldsymbol{\nu}_1[n]\boldsymbol{\nu}_2^*[n] \\ &= e^{jn(\omega_1-\omega_2)} + \boldsymbol{\nu}'[n] + \boldsymbol{\nu}''[n] \end{aligned} \tag{17}$$

where $\mathbb{E}[(\boldsymbol{\nu}'[n])^2] = 2\sigma^2$ and $\mathbb{E}[(\boldsymbol{\nu}''[n])^2] = \sigma^4$. Thus the per-entry SNR of vector $\mathbf{z}$ is $1/\sigma_z^2 = 1/(2\sigma^2 + \sigma^4)$. If

the input SNR is low (e.g., less than 0 dB), the $\sigma^4$ term becomes dominant and the SNR of our frequency difference measurement diminishes drastically. The per-element SNR is therefore a bottleneck that cannot be offset simply by increasing the number of measurements, $M$, because correct estimation of the relative channels is crucial for aligning the measurements. Hence, this low SNR regime should be avoided and per-element SNR must be above a constant threshold for every measurement location.

In MIMO communication, the link budget is typically designed for beamformed communication, ensuring *beamformed* SNR is kept at an adequate, relatively constant level. Consequently, the *per-element* SNR decreases by a factor of $1/N$ as array size $N$ grows large. Therefore, in a practical setting, each calibration measurement must be aggregated over a number of symbols proportional to array size to provide sufficient per-element SNR for frequency difference estimation. The measurement complexity of this scheme is therefore $\mathcal{O}(N)$.

**Piggybacking:** Due to geometric reciprocity, the LOS spatial frequencies, $\{\omega'_m = \omega_m - \omega_1\}$, estimated in the process of calibrating one direction can be reused when calibrating the opposite direction. This allows us to bypass the initial frequency difference estimation step and remove the per-element SNR bottleneck. As shown in our results, this can reduce the SNR requirement for the second calibration procedure by a factor of $N$. In principle, piggybacking can be done in either direction. We may choose to provide frequency estimates obtained in downlink calibration for uplink or vice versa, although, from a practical viewpoint, the former may be more desirable. As mentioned above, transmitter calibration imposes a minimum length (proportional to $N$) on the training sequence in order to orthogonalize the signals on different array elements; whereas receiver calibration does not have a minimum sequence length as long as the required SNR is aggregated. Thus reducing the SNR threshold for uplink calibration can reduce data acquisition time while it may have no such effect on downlink calibration.

**Computational complexity:** The most computationally intensive steps in the proposed algorithm are the compressive channel (or dominant frequency) estimation step and the SVD calculation. For the former, we use the NOMP algorithm which has complexity $\mathcal{O}(N \log N)$, while the complexity of SVD is $\mathcal{O}(MN)$. The overall computational complexity of our scheme is therefore $\mathcal{O}(N \log N + MN)$. Since the algorithm requires a relatively small number of measurements $M$, the computational burden scales near linearly with array size.

## V. Numerical Results

In this section we evaluate the performance of our approach via Monte Carlo simulations. Results are averaged over 100 realizations for each setting. We assume the LOS of all user channels have the same magnitude and model the multipath as one or more paths (specified for each case) with randomly chosen spatial frequencies maintaining a minimum separation of $4\pi/N$ from that of the LOS. Calibration phases and amplitudes are generated uniformly at random over $(0, 2\pi)$ and $(0.8, 1.2)$,

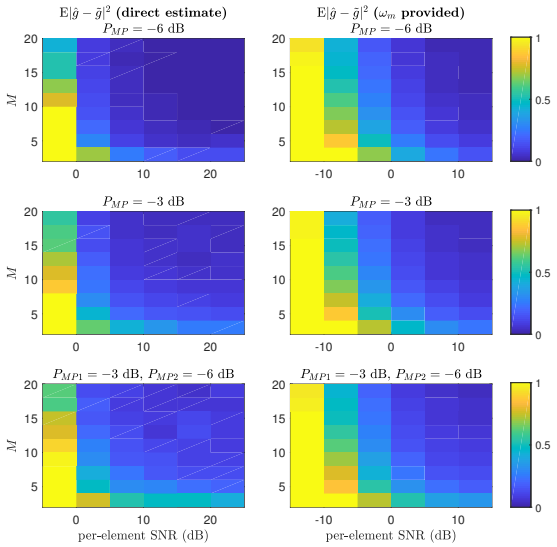


Fig. 3. Performance as a function of aggregate per-element SNR and number of measurements with varying levels of multipath (strengths reported relative to LOS); left: standalone estimate, right: piggybacked estimate.

respectively. As a benchmark, we consider the algorithm of [8] for sensor calibration which relies on second order channel statistics derived from measurement of simultaneous yet independent source transmissions over a long interval. We set the number of sources to 20 and assume the interval is long enough (infinite) to measure the channel covariance exactly. This algorithm assumes single-path channels from all sources and its performance is degraded significantly with even small multipath in the channels. We also report the performance of the standard calibration procedure that assumes measurements from a single source with no multipath (i.e., in an anechoic chamber). We assume noiseless reception for both of these benchmark procedures.

In Fig. 3 we report the normalized beamforming gain obtained using our approach as a function of per-element SNR and number of measurement locations, $M$, for a 100-element receiver with different levels of multipath. It should be noted that these graphs are identical for uplink and downlink calibration assuming the same measurement sequence length and identical transmit power and receiver sensitivity for the user device and base station antenna elements. In this case, the orthogonal sequence transmission and correlation can be abstracted as an identity transform, and there is no meaningful difference between applying the algorithm in uplink and downlink. The results reported in Fig. 3 demonstrate that, with high enough measurement SNR, the algorithm is able to overcome significant multipath with even a small number of measurement locations. We also clearly see the per-element SNR bottleneck described in section IV; at per-element SNR of below 5 dB - corresponding to 25 dB beamformed SNR which is sufficiently high for beamformed communication - the algorithm fails regardless of the number of measurement locations. In the right-hand column graphs, we have plotted the

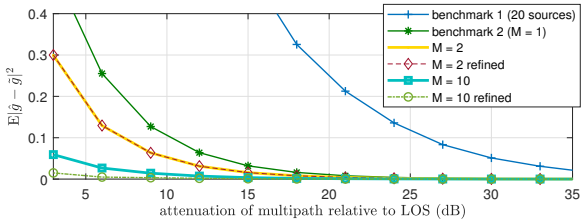


Fig. 4. Performance of proposed algorithm and benchmarks as a function of multipath strength (assuming one multipath component in the channel).

same heatmaps for the case where the initial spatial frequency estimates are supplied from high SNR readings in the opposite direction. In this case, the SNR requirement is significantly lower which confirms our prediction that this first step of estimating the relative LOS spatial frequency offsets is the SNR bottleneck of the algorithm.

Fig. 4 depicts the (noiseless) performance of our algorithm, with and without the refinement step and with different number of measurement locations, against that of the benchmark algorithms. This figure demonstrates clearly the strength of our proposed approach in accurate calibration of arrays in the presence of even the strongest levels of multipath. We also observe that the refinement step can boost performance significantly at high $M$, yet for $M = 2$ there is virtually no gain from refinement. The reason behind this dynamic is that when taking SVD of only 2 measurements, the multipath is not rejected effectively and multipath frequencies seep into our initial estimate, $\hat{\mathbf{g}}$, and consequently cause parasitic frequencies in the compressively reconstructed channel estimate. Without an accurate channel estimate, the refinement step does not improve calibration accuracy, and may even degrade it.

## VI. Conclusions

We presented a technique for post-deployment calibration of MIMO base station transceivers over noisy multipath channels. By aggregating measurements from a diverse set of locations in the cell, the algorithm is able to average out the independent multipath components and emulate a pure LOS channel to measure uplink and downlink calibration offsets. The calibration estimates can further be refined via compressive reconstruction of the full multipath channels that are in turn used to recover more accurate copies of the calibration vector from the raw measurements.

Our simulations demonstrated the robustness of the proposed approach against strong multipath components in the channel, which makes it suitable for on-the-fly calibration in realistic deployment environments. We found that the performance of this algorithm is sensitive to noise power on each antenna element, and therefore the training sequence used for measuring the channel of each source must be long enough to aggregate sufficient per-element SNR. For a typical beamformed communication budget, this length scales linearly with the number of elements in the array, as demonstrated by our numerical results. We also showed, however, that the path reciprocity available to spatially displaced transmitter and receiver arrays can be leveraged to relax this SNR requirement for one of the arrays by piggybacking on the high accuracy channel estimates obtained in the other.

We briefly discussed the added complexity of transmitter calibration, which requires transmission of orthogonal sequences on elements of the transmit array to measure the full channel vectors. In the idealized linear RF chain model assumed here, this process has no effect on the performance of the algorithm as it can be abstracted out as an identity transform; however, in a realistic scenario, nonlinearities in the signal path, such as ADC quantization, amplifier saturation, and dynamic range, can have a significant, assymetrical impact. A detailed treatment of these effects is left for future work.

## References


[1] Ramina Ghods, Alexandra Gallyas-Sanhueza, Seyed Hadi Mirfarshbafan, and Christoph Studer, "BEACHES: Beamspace channel estimation for multi-antenna mmWave systems and beyond," in *2019 IEEE 20th International Workshop on Signal Processing Advances in Wireless Communications (SPAWC)*. IEEE, 2019, pp. 1–5.

[2] Mohammed Abdelghany, Upamanyu Madhow, and Antti Tölli, "Beamspace Local LMMSE: An Efficient Digital Backend for mmWave Massive MIMO," in *2019 IEEE 20th International Workshop on Signal Processing Advances in Wireless Communications (SPAWC)*. IEEE, 2019, pp. 1–5.

[3] Ashok Agrawal and Allan Jablon, "A calibration technique for active phased array antennas," in *IEEE International Symposium on Phased Array Systems and Technology, 2003.* IEEE, 2003, pp. 223–228.

[4] Boon Chong Ng and Chong Meng Samson See, "Sensor-array calibration using a maximum-likelihood approach," *IEEE Transactions on Antennas and Propagation*, vol. 44, no. 6, pp. 827–835, 1996.

[5] Guizhou Wu, Min Zhang, and Fucheng Guo, "On the use of a calibration emitter for direct position determination with single moving array in the presence of sensor gain and phase errors," *Digital Signal Processing*, p. 102734, 2020.

[6] Haralabos Papadopoulos, Ozgun Y Bursalioglu, and Giuseppe Caire, "Avalanche: Fast RF calibration of massive arrays," in *2014 IEEE Global Conference on Signal and Information Processing (GlobalSIP)*. IEEE, 2014, pp. 607–611.

[7] Krishnaprasad Nambur Ramamohan, Sundeep Prabhakar Chepuri, Daniel Fernández Comesaña, and Geert Leus, "Blind sensor array calibration and DOA estimation of broadband sources," in *2019 53rd Asilomar Conference on Signals, Systems, and Computers*. IEEE, 2019, pp. 1304–1308.

[8] Arogyaswami Paulraj and Thomas Kailath, "Direction of arrival estimation by eigenstructure methods with unknown sensor gain and phase," in *ICASSP'85. IEEE International Conference on Acoustics, Speech, and Signal Processing*. IEEE, 1985, vol. 10, pp. 640–643.

[9] Richard Roy and Thomas Kailath, "ESPRIT-estimation of signal parameters via rotational invariance techniques," *IEEE Transactions on acoustics, speech, and signal processing*, vol. 37, no. 7, pp. 984–995, 1989.

[10] Yonina C Eldar, Wenjing Liao, and Sui Tang, "Sensor calibration for off-the-grid spectral estimation," *Applied and Computational Harmonic Analysis*, vol. 48, no. 2, pp. 570–598, 2020.

[11] Tarik Kazaz, Mario Coutino, Gerard JM Janssen, and Alle-Jan van der Veen, "Joint blind calibration and time-delay estimation for multiband ranging," in *ICASSP 2020-2020 IEEE International Conference on Acoustics, Speech and Signal Processing (ICASSP)*. IEEE, 2020, pp. 4846–4850.

[12] Çağdaş Bilen, Gilles Puy, Rémi Gribonval, and Laurent Daudet, "Convex optimization approaches for blind sensor calibration using sparsity," *IEEE Transactions on Signal Processing*, vol. 62, no. 18, pp. 4847–4856, 2014.

[13] Babak Mamandipoor, Dinesh Ramasamy, and Upamanyu Madhow, "Newtonized orthogonal matching pursuit: Frequency estimation over the continuum," *IEEE Transactions on Signal Processing*, vol. 64, no. 19, pp. 5066–5081, 2016.